

A Bayesian Approach to Policy Recognition and State Representation Learning

Adrian Šošić, Abdelhak M. Zoubir and Heinz Koepl

Abstract—Learning from demonstration (LfD) is the process of building behavioral models of a task from demonstrations provided by an expert. These models can be used e.g. for system control by generalizing the expert demonstrations to previously unencountered situations. Most LfD methods, however, make strong assumptions about the expert behavior, e.g. they assume the existence of a deterministic optimal ground truth policy or require direct monitoring of the expert’s controls, which limits their practical use as part of a general system identification framework. In this work, we consider the LfD problem in a more general setting where we allow for arbitrary stochastic expert policies, without reasoning about the quality of the demonstrations. In particular, we focus on the problem of *policy recognition*, which is to extract a system’s latent control policy from observed system behavior. Following a Bayesian methodology allows us to consider various sources of uncertainty about the expert behavior, including the latent expert controls, to model the full posterior distribution of expert controllers. Further, we show that the same methodology can be applied in a nonparametric context to reason about the complexity of the state representation used by the expert and to learn task-appropriate partitions of the system state space.

Index Terms—learning from demonstration, policy recognition, imitation learning, Bayesian nonparametric modeling, Markov chain Monte Carlo, Gibbs sampling, distance dependent Chinese restaurant process



1 INTRODUCTION

LEARNING FROM DEMONSTRATION (LfD) has become a viable alternative to classical reinforcement learning as a new data-driven learning paradigm for building behavioral models based on demonstration data. By exploiting the domain knowledge provided by an expert demonstrator, LfD-built models can focus on the relevant parts of a system’s state space [1] and hence avoid the need of tedious exploration steps performed by reinforcement learners, which often require an impractically high number of interactions with the system environment [2], and always come with the risk of letting the system run into undesired or unsafe states [3]. In addition to that, the learned models have been shown to outperform the expert in several experiments by generalizing from the demonstration data [4], [5], [6].

However, most existing LfD methods come with strong requirements that limit their practical use in real-world scenarios. In particular, they often require direct monitoring of the expert’s controls (e.g. [5], [7], [8]) which is possible only under laboratory-like conditions, or they need to interact with the target system via a simulator, if not by controlling the system directly (see e.g. [9]). Moreover, many methods are restricted to problems with discrete state or action spaces (such as [10]), or they compute only point estimates of the relevant system parameters without providing any information about their level of confidence. Last but not least, the expert is typically assumed to follow an optimal deterministic policy (see e.g. [11]) or to at least approximate one, based on some presupposed degree of confidence in the optimal behavior (as in [12]). While such an assumption may be

reasonable in some situations (e.g. for problems in robotics involving a human demonstrator [1]), it is not appropriate in many others, such as in partially observable environments, where an optimal deterministic policy might not even exist. In fact, Singh et al. [13] showed that, in a general partially observable Markov decision process (POMDP), the best deterministic policy can be arbitrarily worse than the best stochastic one, an argument which also holds in general for multi-agent systems [14]. However, there are even more situations, in which the assumption of a deterministic expert policy is violated. Considering the LfD problem from a more general system identification perspective, our goal could be, for instance, to detect the misbehavior of a dysfunctional agent who has only partial control over its actions and therefore behaves systematically suboptimally. Finally, there are situations, in which we might not even want to reason about the optimality of the demonstrations as, for instance, in the case where we wish to study the exploration strategy of an agent who models its environment (or the reactions of other agents [15]) by randomly triggering different events. In all these cases, existing LfD methods can at best approximate the behavior of the expert as they presuppose the existence of some underlying deterministic ground truth policy.

In this work, we present a novel approach to the LfD problem, in order to address some of the above-mentioned shortcomings of previous methods. Central to our work is the problem of *policy recognition*, that is, to extract an arbitrary system’s policy from observations of its behavior. Herein, our goal is to make as few assumptions about the expert behavior policy as possible and, thus, we consider the whole class of stochastic expert policies, without ever reasoning about the optimality of the demonstrations. All in all, our objective in this paper is twofold: we not only attempt to answer the question *how* the expert solves a given

• All authors are with the Department of Electrical Engineering and Information Technology, Technische Universität Darmstadt, Germany

task but also to infer *which information* is used by the expert to solve it. This knowledge is captured in the form of a joint posterior distribution over possible expert state representations and corresponding state controllers. By learning the underlying state representation of the expert, our approach is essentially comparable to partially observable models in that we infer the latent observation space of the expert, together with a corresponding functional mapping from the system state space. As the complexity of the observation space is unknown *a priori*, we finally present a Bayesian nonparametric approach to explore the underlying structure of the space based on the available demonstration data.

1.1 Problem statement

Given a set of expert demonstrations in the form of a system trajectory $\mathbf{s} = (s_1, s_2, \dots, s_T) \in \mathcal{S}^T$ of length T , where \mathcal{S} denotes the system state space, our goal is to determine the latent control policy used by the expert to generate the state sequence.¹ For this problem, we follow the general Markov decision process (MDP) formalism [16] as the underlying framework describing the dynamical properties of our system. In particular, we consider a reduced MDP $(\mathcal{S}, \mathcal{A}, \mathcal{T}, \pi)$ which consists of the discrete or continuous state space \mathcal{S} , a discrete set of actions \mathcal{A} containing $|\mathcal{A}|$ elements, a transition model $\mathcal{T} : \mathcal{S} \times \mathcal{S} \times \mathcal{A} \rightarrow \mathbb{R}$ where $\mathcal{T}(s' | s, a)$ denotes the probability of reaching s' after taking action a in state s , and a policy π modeling the expert's choice of actions.² In the sequel, we assume that the policy is parametrized by some parameter $\omega \in \Omega$, called the *global control parameter* of the system, and we denote by $\pi(a | s, \omega)$ the probability that the expert performs action a in state s , i.e. $\pi : \mathcal{S} \times \mathcal{A} \times \Omega \rightarrow [0, 1]$. The set Ω is called the parameter space of the policy, which specifies the class of feasible action distributions. The specific form of Ω depends on the particular model used and will be discussed later.

Using a parametric description for π is convenient as it shifts the policy recognition task from determining the possibly infinite set of *local policies* at all states in \mathcal{S} (i.e. the set of all state-conditional action distributions) to inferring the posterior distribution $p(\omega | \mathbf{s})$,

$$p(a | s_0, \mathbf{s}) = \int_{\Omega} \pi(a | s_0, \omega) p(\omega | \mathbf{s}) d\omega,$$

where $s_0 \in \mathcal{S}$ is some arbitrary query point. Since the local policies are coupled through the global control parameter ω as indicated by the above integral equation, inferring ω not only means to determine the individual local policies but also their (spatial) dependencies. Learning the structure of ω from observation data thus also provides a way to learn a problem-specific state representation of the task performed by the expert. This relationship will be discussed in detail in the forthcoming sections.

For the remainder of this paper, we assume that the transition model \mathcal{T} as well as the system state space \mathcal{S} and the action set \mathcal{A} are known. The assumption of knowing \mathcal{S} follows naturally, as we already assumed we can observe

the expert acting in \mathcal{S} . In the proposed Bayesian framework, the latter assumption can be easily relaxed by allowing for noisy or incomplete trajectory data. However, as this would not provide additional insights into the main principles of our method, we do not consider such an extension in this work.

The assumption of knowing the transition dynamics \mathcal{T} is a simplifying one but prevents us from running into model identifiability problems: if we do not constrain our system transition model in some way, any observed state transition in \mathcal{S} could be trivially explained by a corresponding local adaptation of the assumed model \mathcal{T} and, thus, there would be little hope to extract the true expert policy from the observation data. Assuming a fixed transition model is the easiest way to resolve this model ambiguity. However, there are other alternatives, such as using a parametrized family of transition models, which we leave for future work. Nevertheless, it should be mentioned that our proposed inference algorithm naturally processes the observation data piecewise in the form of one-step state transitions $\{(s_t, s_{t+1})\}$, meaning that we can tolerate deviations from the true system dynamics as long as the model \mathcal{T} is sufficiently accurate to extract some (local) information about the corresponding action a_t , taken by the expert (see details in Section 2). This is in contrast to planning-based approaches, where small modeling errors in the dynamics can accumulate and yield consistently wrong policy results [8], [19].

The requirement of knowing the action set \mathcal{A} is less stringent: if \mathcal{A} is unknown *a priori*, we may simply assume a potentially rich class of actions, as long as the transition model \mathcal{T} can provide the corresponding dynamics. Figuring out which of the hypothetical actions are actually performed by the expert and, more importantly, how they are used, shall be the task of our inference algorithm.

1.2 Related work

The idea of learning from demonstration has now been around for several decades. Most of the work on LfD has been presented by the robotics community (see [1] for a survey), but recent advances in the field have triggered developments in other research areas as well, such as in cognitive science [20] and human-machine interaction [21]. Depending on the particular setup, the problem is sometimes referred to as imitation learning [22], apprenticeship learning [9], inverse reinforcement learning [11], inverse optimal control [23], preference elicitation [20], plan recognition [24] or behavioral cloning [5]. What makes our *policy recognition* framework fundamentally different from the above is the fact that we formulate the learning problem in a way which is *not* restricted to a certain class of ground truth policies (e.g. deterministic or softmax policies [12]). Moreover, our inference machinery is entirely passive, which means that we require no active control of the target system or access to the actions performed by the expert. A more detailed comparison to existing frameworks is presented in Section 6.

Most of the above LfD models can be either categorized as intentional models (such as inverse reinforcement learning models), or sub-intentional models (e.g. behavioral cloning models). While the latter class only predicts an agent's behavior via a learned policy representation, intentional models also attempt to capture the agent's beliefs

1. The generalization to multiple trajectories is straightforward as they are conditionally independent given the system parameters.

2. This reduced model is sometimes referred to as an MDP\(\mathbb{R}\) (see e.g. [9], [17], [18]) to emphasize the nonexistence of a reward function.

and intentions, e.g. in the form of a reward function. Consequently, intentional models are often considered to have better generalization abilities³ but they typically require a certain amount of task-specific prior information in order to resolve the ambiguous relationship between intention and behavior (i.e. there are often many ways to solve a certain task [11]). Also, though they are interesting from a psychological point of view [20], intentional models target a much harder problem than what is actually required in many LfD scenarios. For instance, it is not always necessary to understand an agent’s intention if we only wish to (locally) match its behavior. Sub-intentional models, on the other hand, often reduce the LfD problem to a simplistic supervised setting, typically ignoring the possibly stochastic nature of the expert behavior.

Answering the question whether or not an intention-based modeling of the LfD problem is advantageous is out of the scope of this paper; however, we point to the detailed discussion in [25]. Rather, we focus on the policy recognition task and present a hybrid solution, containing both intentional and sub-intentional elements. More specifically, we do not model the experts goals but try to learn a task-specific representation of the system state space to facilitate the policy prediction task.

1.3 Paper outline

The outline of the paper is as follows: in Section 2, we introduce our parametric policy recognition framework and derive inference algorithms for both discrete and continuous state spaces. In Section 3, we consider the policy recognition problem from a nonparametric viewpoint and provide some insights into the state representation learning problem. In Section 4, we discuss some special issues arising in continuous spaces. Simulation results are presented in Section 5 and a final discussion of related work can be found in Section 6.

2 PARAMETRIC POLICY RECOGNITION

2.1 Finite state spaces: the static model

First, let us assume that our system can be modeled on a finite state space \mathcal{S} and let $|\mathcal{S}|$ denote its cardinality. For notational convenience, we represent states and actions by integer values. Starting with the most general case, we assume that the agent uses an individual control strategy for each state. Accordingly, we introduce a corresponding control parameter θ_i for each $i \in \{1, \dots, |\mathcal{S}|\}$, called the *local control parameter* at state i , by which the agent controls the actions being performed at i . More formally, we model the played action as a categorical random variable and let the j^{th} element of θ_i represent the probability of executing action j at state i . Consequently, θ_i lies in the $(|\mathcal{A}| - 1)$ -simplex, which we in the sequel denote by the symbol Δ for brevity of notation, i.e. $\theta_i \in \Delta \subset \mathbb{R}^{|\mathcal{A}|}$. Summarizing all local control parameters in a single matrix, $\Theta \in \Delta^{|\mathcal{S}|} =: \Omega$, we obtain the *global control parameter* of the system as introduced in Section 1.1, which fully specifies the agent

3. The rationale is that an agent’s intention is always specific to the task being performed and can hence serve as its compact description [11]. However, if the intention of the agent is misunderstood, then also the subsequent generalization step will trivially fail.

behavior in terms of its vectors $\{\theta_i\}_{i=1}^{|\mathcal{S}|}$. Note that the global control parameter is here denoted by Θ instead of ω , for reasons that will become clear later. Each action a is then characterized by the policy induced by the respective local control of the underlying state, i.e.

$$\pi(a \mid s = i, \Theta) = \text{CAT}(a \mid \theta_i).$$

For simplicity, we will write $\pi(a \mid \theta_i)$ since the state i is used only to select the appropriate local control parameter for the current state.

Given the finite action set \mathcal{A} , it is convenient to place a (symmetric) Dirichlet prior on the local controls, i.e.

$$p_\theta(\theta_i \mid \alpha) = \text{DIR}(\theta_i \mid \alpha \cdot \mathbf{1}^{|\mathcal{A}|}),$$

since the Dirichlet distribution is conjugate to the categorical distribution over actions.⁴ Here, $\mathbf{1}^{|\mathcal{A}|}$ denotes a vector of all ones of length $|\mathcal{A}|$. The prior is itself parametrized by a concentration parameter α which can be further described by a hyperprior $p_\alpha(\alpha)$, giving rise to a Bayesian hierarchical model. For simplicity, we assume the value of α to be known for the remainder of this paper, though an extension to a full Bayesian treatment is straightforward. The joint distribution of all model variables is then given as

$$\begin{aligned} p(\mathbf{s}, \mathbf{a}, \Theta \mid \alpha) &= p_1(s_1) \prod_{i=1}^{|\mathcal{S}|} p_\theta(\theta_i \mid \alpha) \dots & (1) \\ &\dots \times \prod_{t=1}^{T-1} \mathcal{T}(s_{t+1} \mid s_t, a_t) \pi(a_t \mid \theta_{s_t}), \end{aligned}$$

where $\mathbf{a} = (a_1, a_2, \dots, a_{T-1})$ is the latent action sequence taken by the agent, and $p_1(\cdot)$ denotes the initial state distribution of the system. The corresponding graphical model is depicted in Fig. 1 (ignoring the \mathbf{z} variable). Throughout the rest of the paper, we refer to it as the *static model*.

In the sequel, our goal is to approximate the posterior distribution $p(\Theta \mid \mathbf{s}, \alpha)$, which contains all information that is necessary to make predictions about the expert behavior.

2.1.1 Gibbs sampling

In a Bayesian approach, the expert’s actions need to be marginalized out during the inference process as they correspond to unobserved variables. This can be done by first approximating the joint posterior distribution $p(\Theta, \mathbf{a} \mid \mathbf{s}, \alpha)$ over both controls and actions, using a finite number of Q samples, and then marginalizing over \mathbf{a} in a second step,

$$\begin{aligned} p(\Theta \mid \mathbf{s}, \alpha) &= \sum_{\mathbf{a}} p(\Theta, \mathbf{a} \mid \mathbf{s}, \alpha) & (2) \\ &\approx \sum_{\mathbf{a}} \left(\frac{1}{Q} \sum_{q=1}^Q \delta_{\Theta^{\{q\}} \mathbf{a}^{\{q\}}}(\Theta, \mathbf{a}) \right) = \frac{1}{Q} \sum_{q=1}^Q \delta_{\Theta^{\{q\}}}(\Theta), \end{aligned}$$

where $\Theta^{\{q\}}, \mathbf{a}^{\{q\}} \sim p(\Theta, \mathbf{a} \mid \mathbf{s}, \alpha)$, and $\delta_x(\cdot)$ denotes Dirac’s delta function centered at x . The fact that we first approximate the joint posterior distribution and then drop the action samples allows for a simple inference procedure since the joint samples $\{\Theta^{\{q\}}, \mathbf{a}^{\{q\}}\}_{q=1}^Q$ can be easily generated using a Gibbs sampling scheme. More specifically,

4. It should be pointed out that the framework also applies for deterministic expert policies by changing the prior distribution accordingly.

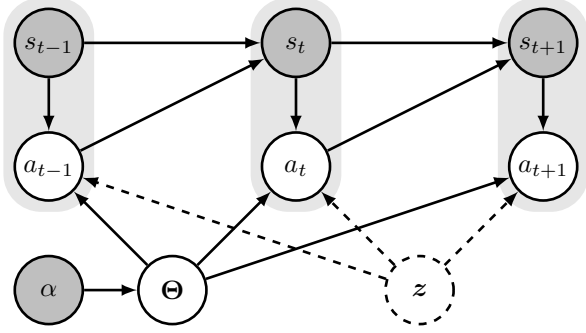


Fig. 1: Graphical model of our policy recognition framework. The underlying dynamical structure is that of an MDP whose global control parameter Θ is treated as a random variable with prior distribution parametrized by α . The indicator node z is used for the clustering model in Section 2.2. Observed variables are highlighted in gray.

they are obtained by sampling iteratively from the following two conditional distributions, which can be derived directly from the joint model (1),

$$p(a_t | \mathbf{a}_{-t}, \mathbf{s}, \Theta, \alpha) \propto \mathcal{T}(s_{t+1} | s_t, a_t) \pi(a_t | \theta_{s_t}),$$

$$p(\theta_i | \Theta_{-i}, \mathbf{s}, \mathbf{a}, \alpha) \propto p_\theta(\theta_i | \alpha) \prod_{t: s_t=i} \pi(a_t | \theta_i).$$

Here, \mathbf{a}_{-t} and Θ_{-i} refer to all actions/controls except a_t and θ_i , respectively. The latter of the two expressions reveals that, in order to sample θ_i , we need to consider only those actions played at the corresponding state i . Furthermore, the first expression shows that, given Θ , all actions $\{a_t\}$ can be sampled independently from each other. Therefore, inference can be done in parallel for all θ_i . This can also be seen from the fact that the posterior of the global control parameter factorizes over states, i.e.

$$p(\Theta | \mathbf{s}, \mathbf{a}, \alpha) \propto \prod_{i=1}^{|S|} p_\theta(\theta_i | \alpha) \prod_{t: s_t=i} \pi(a_t | \theta_i). \quad (3)$$

From the conjugacy of $p_\theta(\theta_i | \alpha)$ and $\pi(a_t | \theta_i)$, it follows that the posterior over θ_i is again Dirichlet distributed with updated concentration parameter. In particular, denoting by $\phi_{i,j}$ the number of times that action j is played at state i for a given assignment of actions \mathbf{a} , i.e.

$$\phi_{i,j} := \sum_{t: s_t=i} \mathbb{1}(a_t = j), \quad (4)$$

and by collecting these values in the form of vectors, $\phi_i := [\phi_{i,1}, \dots, \phi_{i,|A|}]$, we can re-write Eq. (3) as

$$p(\Theta | \mathbf{s}, \mathbf{a}, \alpha) = \prod_{i=1}^{|S|} \text{DIR}(\theta_i | \phi_i + \alpha \cdot \mathbf{1}^{|A|}). \quad (5)$$

2.1.2 Collapsed Gibbs sampling

Choosing a Dirichlet distribution as prior model for the local control parameters is convenient as it allows us to arrive at analytic expressions for the conditional distributions that are required to run the Gibbs sampler. As an alternative, we can exploit the conjugacy property of $p_\theta(\theta_i | \alpha)$ and $\pi(a_t | \theta_i)$ to marginalize out the control parameters during

the sampling process, giving rise to a collapsed sampling scheme. Collapsed sampling is advantageous in two different respects: 1) it reduces the total number of variables to be sampled and therewith the number of computations required per Gibbs iteration 2) it increases the mixing speed of the underlying Markov chain that governs the sampling process, reducing the correlation of the obtained samples and therewith the variance of the resulting policy estimate.

Formally, collapsing means that we no longer use a sample representation for $p(\Theta, \mathbf{a} | \mathbf{s}, \alpha)$ as in Eq. (2), but instead approximate the marginal density $p(\mathbf{a} | \mathbf{s}, \alpha)$,

$$p(\Theta | \mathbf{s}, \alpha) = \sum_{\mathbf{a}} p(\Theta | \mathbf{s}, \mathbf{a}, \alpha) p(\mathbf{a} | \mathbf{s}, \alpha) \quad (6)$$

$$\approx \sum_{\mathbf{a}} p(\Theta | \mathbf{s}, \mathbf{a}, \alpha) \left(\frac{1}{Q} \sum_{q=1}^Q \delta_{\mathbf{a}^{(q)}}(\mathbf{a}) \right)$$

$$= \frac{1}{Q} \sum_{q=1}^Q p(\Theta | \mathbf{s}, \mathbf{a}^{(q)}, \alpha),$$

where $\mathbf{a}^{(q)} \sim p(\mathbf{a} | \mathbf{s}, \alpha)$. In contrast to the previous approach, the target distribution is thus no longer represented by a sum of Dirac measures but described by a Dirichlet mixture (c.f. Eq. (5)). The required samples $\{\mathbf{a}^{(q)}\}_{q=1}^Q$ can be obtained by running a collapsed Gibbs sampler with

$$p(a_t | \mathbf{a}_{-t}, \mathbf{s}, \alpha) \propto \int_{\Delta^{|S|}} p(\mathbf{s}, \mathbf{a}, \Theta | \alpha) d\Theta$$

$$\propto \mathcal{T}(s_{t+1} | s_t, a_t) \int_{\Delta} p_\theta(\theta_{s_t} | \alpha) \prod_{t': s_{t'}=s_t} \pi(a_{t'} | \theta_{s_t}) d\theta_{s_t}.$$

It turns out that the above distribution allows for a simple sampling mechanism since the integral part, when viewed as a function of action a_t only, can be identified as the conditional of a Dirichlet-multinomial distribution. This distribution is then re-weighted by the likelihood $\mathcal{T}(s_{t+1} | s_t, a_t)$ of the observed transition. The final (unnormalized) weights of the resulting categorical distribution are hence given as

$$p(a_t = j | \mathbf{a}_{-t}, \mathbf{s}, \alpha) \propto \mathcal{T}(s_{t+1} | s_t, a_t = j) \cdot (\varphi_{t,j} + \alpha), \quad (7)$$

where $\varphi_{t,j}$ counts the number of occurrences of action j among all actions in \mathbf{a}_{-t} played at the same state as a_t (that is, s_t). Explicitly,

$$\varphi_{t,j} := \sum_{\substack{t': s_{t'}=s_t \\ t' \neq t}} \mathbb{1}(a_{t'} = j).$$

Note that these values can also be expressed in terms of the sufficient statistics introduced in the last section, i.e.

$$\varphi_{t,j} = \phi_{s_t,j} - \mathbb{1}(a_t = j).$$

As before, actions being played at different states can be sampled independently from each other (see Eq. (7)) because they are governed by different local control parameters. Consequently, inference about Θ again decouples for all states.

Finally, it should be pointed out that we can also arrive at a mixture representation for the ordinary Gibbs sampler described in Section 2.1.1 by dropping the sampled controls $\{\Theta^{(q)}\}$ instead of $\{\mathbf{a}^{(q)}\}$, which can be beneficial in cases where we require a smooth description of the posterior. This

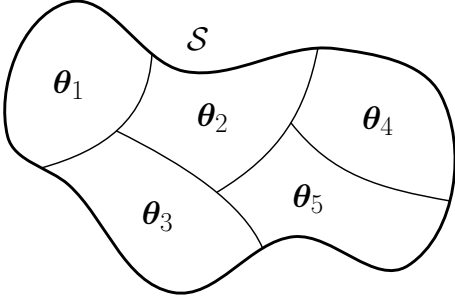


Fig. 2: Schematic illustration of the clustering approach. The state space \mathcal{S} is partitioned into a set of clusters $\{\mathcal{C}_k\}$, each governed by its individual local control parameter θ_k .

is possible since the limiting marginal distribution of each action sample $\mathbf{a}^{\{q\}}$ is $p(\mathbf{a} \mid \mathbf{s}, \alpha)$, and hence Eq. (6) applies.

2.2 Towards infinite spaces: a clustering approach

While the methodology introduced so far provides a means to solve the policy recognition problem in finite state spaces, the presented approaches quickly become infeasible for large spaces as, in the continuous limit, the number of parameters to be learned (i.e. the size of Θ) will grow unbounded with the size of the space. In that sense, the presented methodology is prone to overfitting for larger problems as we will never have enough data to cover the whole system state space. Furthermore, as the model makes no assumptions about the structure of Θ but treats all local policies separately (c.f. Eq. (5)), we are not able to generalize to regions of the state space that are not directly visited by the expert. Yet, we would certainly like to predict the expert behavior also at states for which there is no trajectory data available and, moreover, we should be able to expect a well-designed model to produce increasingly accurate predictions at regions closer to the observed trajectories (with the precise definition of “closeness” being left open for the moment).

A simple way to counteract the overfitting problem in general, is to restrict the complexity of a model by limiting the number of free parameters. In our case, we can avoid the parameter space to grow unbounded by considering a finite number of local policies to be shared among the states. In the sequel, we thus assume that the agent chooses among K local controllers with corresponding parameters $\{\theta_k\}_{k=1}^K$. Accordingly, we introduce a set of indicator or cluster assignment variables, $\{z_i\}_{i=1}^{|\mathcal{S}|}$, one for each state of the state space, which map the states to their corresponding local control parameters (see Fig. 1). Obviously, such an assignment implies a partitioning of the state space (see Fig. 2), resulting in the following K clusters,

$$\mathcal{C}_k := \{i : z_i = k\}, \quad k \in \{1, \dots, K\}.$$

Although we motivated the clustering of states by the overfitting problem, partitioning the system space seems not only convenient from an inference point of view. In fact, mapping the problem down to a lower-dimensional space is also reasonable for practical reasons as we are typically interested in understanding an agent’s behavior on a certain

finite scale, that is, with a spatially finite precision. This can be explained by the following reasons:

- In practice, the observed trajectory data will always be noisy since we can take our measurements only up to a certain finite precision. Therefore, even though we do not explicitly model the observation noise in our framework, clustering the data appears reasonable in order to robustify the model against small perturbations in the observations.
- Considering the system from a control perspective, the complexity of subsequent planning steps can be potentially reduced if the system dynamics can be approximately described on a lower-dimensional manifold of the state space, meaning that the system behavior can be well represented by a smaller set of informative states (c.f. finite state controllers [26]). The LfD problem can then be reduced to learning a near-optimal controller based on a small set of local policies that together provide a good approximation of the global agent behavior. What remains, is the question how we can find such a representation. The clustering approach described above offers one possible solution to this problem.
- Finally, in any real setup, it is most reasonable to assume that the expert itself can only execute a finite-precision policy due to its own limited sensing abilities of the space. Consequently, the demonstrated behavior is going to be optimal only up to a certain finite precision, as the agent is generally not able to discriminate between arbitrary small differences of states. An interesting question in this context is whether we can infer the underlying state representation of the agent by observing his reactions to the environment in the form of the resulting state trajectory. We will discuss this issue in detail in Section 3.

By introducing the cluster assignment variables $\{z_i\}_{i=1}^{|\mathcal{S}|}$, the joint distribution in Eq. (1) changes into

$$p(\mathbf{s}, \mathbf{a}, \mathbf{z}, \Theta \mid \alpha) = p_1(s_1) \prod_{k=1}^K p_\theta(\theta_k \mid \alpha) \dots \\ \dots \times \prod_{t=1}^{T-1} \mathcal{T}(s_{t+1} \mid s_t, a_t) \pi(a_t \mid \theta_{z_{s_t}}) p_z(\mathbf{z}),$$

where $\mathbf{z} = (z_1, z_2, \dots, z_{|\mathcal{S}|})$ denotes the collection of all indicator variables and $p_z(\mathbf{z})$ is the corresponding prior distribution to be further discussed in Section 2.2.3. Note that the static model can be recovered as a special case of the above when each state describes its own cluster, i.e. by setting $K = |\mathcal{S}|$ and fixing $z_i = i$ (hence the name *static*).

In contrast to the static model, we now require both the indicator z_i and the corresponding local control parameter θ_{z_i} in order to characterize the agent’s behavior at a given state i . Accordingly, the global control parameter of the model is $\omega = (\Theta, \mathbf{z})$ with corresponding parameter space $\Omega \subset \Delta^K \times \{1, \dots, K\}^{|\mathcal{S}|}$, and our target distribution becomes $p(\Theta, \mathbf{z} \mid \mathbf{s}, \alpha)$. In what follows, we derive both the Gibbs and the collapsed Gibbs sampler as mechanisms for approximate inference in this setting.

2.2.1 Gibbs sampling

Unsurprisingly, the expressions for the conditionals over actions and controls take a similar form to those of the static model, with the only difference that we no longer group the

actions by their states but according to their generating local policies or, equivalently, the clusters $\{\mathcal{C}_k\}$. In particular,

$$\begin{aligned} p(a_t | \mathbf{a}_{-t}, \mathbf{s}, \mathbf{z}, \Theta, \alpha) &\propto \mathcal{T}(s_{t+1} | s_t, a_t) \cdot \pi(a_t | \boldsymbol{\theta}_{z_{s_t}}), \\ p(\boldsymbol{\theta}_k | \Theta_{-k}, \mathbf{s}, \mathbf{a}, \mathbf{z}, \alpha) &\propto p_\theta(\boldsymbol{\theta}_k | \alpha) \prod_{t:z_{s_t}=k} \pi(a_t | \boldsymbol{\theta}_k) \\ &\propto p_\theta(\boldsymbol{\theta}_k | \alpha) \prod_{t:s_t \in \mathcal{C}_k} \pi(a_t | \boldsymbol{\theta}_k). \end{aligned}$$

The latter expression again takes the form of a Dirichlet distribution with updated concentration parameter, i.e.

$$p(\boldsymbol{\theta}_k | \Theta_{-k}, \mathbf{s}, \mathbf{a}, \mathbf{z}, \alpha) = \text{DIR}(\boldsymbol{\theta}_k | \boldsymbol{\xi}_k + \alpha \cdot \mathbf{1}^{|\mathcal{A}|}),$$

where $\boldsymbol{\xi}_k := [\xi_{k,1}, \dots, \xi_{k,|\mathcal{A}|}]$, and $\xi_{k,j}$ denotes the number of times that action j is played at states belonging to cluster \mathcal{C}_k in the given assignment of \mathbf{a} . Explicitly,

$$\xi_{k,j} := \sum_{t:z_{s_t}=k} \mathbb{1}(a_t = j) = \sum_{i \in \mathcal{C}_k} \sum_{t:s_t=i} \mathbb{1}(a_t = j), \quad (8)$$

which is nothing but the sum of the $\phi_{i,j}$'s of the corresponding states, i.e.

$$\xi_{k,j} = \sum_{i \in \mathcal{C}_k} \phi_{i,j}.$$

In addition to the action and control variables, we now also need to sample the indicators $\{z_i\}_{i=1}^{|S|}$, whose conditional distributions can be expressed in terms of the prior model and the likelihood of the triggered actions, i.e.

$$p(z_i | \mathbf{z}_{-i}, \mathbf{s}, \mathbf{a}, \Theta, \alpha) \propto p(z_i | \mathbf{z}_{-i}) \prod_{t:s_t=i} \pi(a_t | \boldsymbol{\theta}_{z_i}). \quad (9)$$

2.2.2 Collapsed Gibbs sampling

As before, we derive the corresponding collapsed sampler by marginalizing out the control parameters, i.e.

$$\begin{aligned} p(z_i | \mathbf{z}_{-i}, \mathbf{s}, \mathbf{a}, \alpha) &\propto \int_{\Delta^K} p(\mathbf{s}, \mathbf{a}, \mathbf{z}, \Theta | \alpha) d\Theta \\ &\propto p(z_i | \mathbf{z}_{-i}) \int_{\Delta^K} \prod_{k=1}^K p_\theta(\boldsymbol{\theta}_k | \alpha) \prod_{t=1}^{T-1} \pi(a_t | \boldsymbol{\theta}_{z_{s_t}}) d\Theta \\ &\propto p(z_i | \mathbf{z}_{-i}) \int_{\Delta^K} \prod_{k=1}^K p_\theta(\boldsymbol{\theta}_k | \alpha) \prod_{i'=1}^{|S|} \prod_{t:s_t=i'} \pi(a_t | \boldsymbol{\theta}_{z_{i'}}) d\Theta \\ &\propto p(z_i | \mathbf{z}_{-i}) \int_{\Delta^K} \prod_{k=1}^K p_\theta(\boldsymbol{\theta}_k | \alpha) \prod_{i':z_{i'}=k} \prod_{t:s_t=i'} \pi(a_t | \boldsymbol{\theta}_k) d\Theta \\ &\propto p(z_i | \mathbf{z}_{-i}) \prod_{k=1}^K \left(\int_{\Delta} p_\theta(\boldsymbol{\theta}_k | \alpha) \prod_{t:s_t \in \mathcal{C}_k} \pi(a_t | \boldsymbol{\theta}_k) d\boldsymbol{\theta}_k \right). \end{aligned} \quad (10)$$

Here, we first grouped the actions by their associated states and then grouped the states themselves by the clusters $\{\mathcal{C}_k\}$. Again, this distribution admits an easy sampling mechanism as it takes the form of a product of Dirichlet-multinomials, re-weighted by the conditional prior distribution over indicators. In particular, we observe that all actions played at some state i appear in exactly one of the K integrals of the last equation. In other words, by changing the value of z_i , i.e. by assigning state i to another cluster, only two of the involved integrals will change: the one belonging to the previously assigned cluster and the one of

the new cluster. Inference about the value of z_i can therefore be carried out using the following two sets of sufficient statistics:

- $\phi_{i,j}$: the number of actions j played at state i ,
- $\psi_{i,j,k}$: the number of actions j played at states assigned to cluster \mathcal{C}_k , excluding state i .

The $\phi_{i,j}$'s are the same as in Eq. (4) and their definition is repeated here just as a reminder. For the $\psi_{i,j,k}$'s, on the other hand, we find the following explicit expression,

$$\psi_{i,j,k} := \sum_{\substack{i' \in \mathcal{C}_k \\ i' \neq i}} \sum_{t:s_t=i'} \mathbb{1}(a_t = j),$$

which can be also written in terms of the statistics used for the ordinary Gibbs sampler, i.e.

$$\psi_{i,j,k} = \xi_{k,j} - \mathbb{1}(i \in \mathcal{C}_k) \cdot \phi_{i,j}.$$

By collecting these quantities in a vector, i.e. $\boldsymbol{\psi}_{i,k} := [\psi_{i,1,k}, \dots, \psi_{i,|\mathcal{A}|,k}]$, we end up with the following simplified expression,

$$\begin{aligned} p(z_i = k | \mathbf{z}_{-i}, \mathbf{s}, \mathbf{a}, \alpha) &\propto p(z_i = k | \mathbf{z}_{-i}) \dots \\ &\dots \times \prod_{k'=1}^K \text{DIRMULT}(\boldsymbol{\psi}_{i,k'} + \mathbb{1}(k' = k) \cdot \boldsymbol{\phi}_i | \alpha). \end{aligned}$$

Further, we obtain the following result for the conditional distribution of action a_t ,

$$\begin{aligned} p(a_t | \mathbf{a}_{-t}, \mathbf{s}, \mathbf{z}, \alpha) &\propto \mathcal{T}(s_{t+1} | s_t, a_t) \dots \\ &\dots \times \int_{\Delta} p_\theta(\boldsymbol{\theta}_{z_{s_t}} | \alpha) \prod_{t':z_{s_{t'}}=z_{s_t}} \pi(a_{t'} | \boldsymbol{\theta}_{z_{s_t}}) d\boldsymbol{\theta}_{z_{s_t}}. \end{aligned}$$

By introducing the sufficient statistics $\{\vartheta_{t,j}\}$ which count the number of occurrences of action j among all states that are currently assigned to the same cluster as s_t (i.e. the cluster $\mathcal{C}_{z_{s_t}}$), excluding a_t itself,

$$\vartheta_{t,j} := \sum_{\substack{t':z_{s_{t'}}=z_{s_t} \\ t' \neq t}} \mathbb{1}(a_{t'} = j),$$

we finally arrive at the following expression,

$$p(a_t = j | \mathbf{a}_{-j}, \mathbf{s}, \mathbf{z}, \alpha) \propto (\vartheta_{t,j} + \alpha) \cdot \mathcal{T}(s_{t+1} | s_t, a_t = j).$$

As for the static model, we can establish a relationship between the statistics used for the ordinary and the collapsed sampler, i.e.

$$\vartheta_{t,j} = \xi_{z_{s_t},j} - \mathbb{1}(a_t = j).$$

2.2.3 Prior models

In order to complete the model, we still need to specify a prior distribution over indicator variables $p_z(\mathbf{z})$. In the sequel, we present three simple candidate models:

Non-informative prior:

The simplest of all prior models is the non-informative prior over partitionings, reflecting the assumption that, *a priori*, all cluster assignments are equally likely and the indicators $\{z_i\}$ are mutually independent. In this case, $p_z(\mathbf{z})$ is constant and hence the term $p(z_i | \mathbf{z}_{-i})$ in Eq. (9) and Eq. (10) disappears so that the posterior distribution of the

indicators is directly proportional to the likelihood of the inferred action sequence.

Mixing prior:

Another simple yet expressive prior can be realized by the (finite) Dirichlet mixture model. Instead of assuming that the indicator variables are independent, the model uses a set of mixing coefficients $\mathbf{q} = [q_1, \dots, q_K]$, where q_k represents the prior probability that an indicator variable takes on value k . The mixing coefficients are themselves modeled by a Dirichlet distribution, so that we finally have

$$\mathbf{q} \sim \text{DIR}(\mathbf{q} \mid \frac{\gamma}{K} \cdot \mathbf{1}^K)$$

$$z_i \mid \mathbf{q} \sim \text{CAT}(z_i \mid \mathbf{q}),$$

with γ being another concentration parameter that controls the variability of the mixing coefficients. Note that the indicator variables are still *conditionally* independent given the mixing coefficients in this model. More specifically, for a fixed \mathbf{q} , the conditional distribution of a single indicator in Eq. (9) and Eq. (10) takes the following simple form, i.e.

$$p(z_i = k \mid z_{-i}, \mathbf{q}) = q_k.$$

If, on the other hand, the value of \mathbf{q} is unknown, we have two options how to include the prior into our framework. One is to sample \mathbf{q} additionally to the remaining variables. For this, we draw elements from the following conditional distribution during the Gibbs sampling procedure,

$$p(\mathbf{q} \mid \mathbf{s}, \mathbf{a}, \mathbf{z}, \Theta, \alpha) \propto \text{DIR}(\mathbf{q} \mid \frac{\gamma}{K} \cdot \mathbf{1}^K) \prod_{i=1}^{|\mathcal{S}|} \text{CAT}(z_i \mid \mathbf{q})$$

$$\propto \text{DIR}(\mathbf{q} \mid \zeta + \frac{\gamma}{K} \cdot \mathbf{1}^K),$$

where $\zeta := [\zeta_1, \dots, \zeta_K]$, and ζ_k denotes the number of variables z_i that map to cluster \mathcal{C}_k , i.e.

$$\zeta_k = \sum_{i=1}^{|\mathcal{S}|} \mathbb{1}(z_i = k).$$

Alternatively, we can again make use of the conjugacy property to marginalize out the mixing proportions \mathbf{q} during the inference process, just as we did for the control parameters in previous sections. The result is (additional) collapsing in \mathbf{q} , depending on whether the sampler in Section 2.2.1 or Section 2.2.2 is used. In both cases, we simply replace the factor $p(z_i = k \mid z_{-i})$ appearing in the conditional of z_i by

$$p(z_i = k \mid z_{-i}, \gamma) \propto (\zeta_k^{(-i)} + \frac{\gamma}{K}), \quad (11)$$

where $\zeta_k^{(-i)}$ is defined like ζ_k without counting the current value of indicator z_i , i.e.

$$\zeta_k^{(-i)} := \sum_{\substack{i'=1 \\ i' \neq i}}^{|\mathcal{S}|} \mathbb{1}(z_{i'} = k) = \zeta_k - \mathbb{1}(z_i = k).$$

A detailed derivation is omitted here but follows the same style as for the collapsing in Section 2.1.2.

Spatial prior:

While both previous models assume (conditional) independence of the indicator variables and hence make no assumptions about their dependency structure, we can also use the

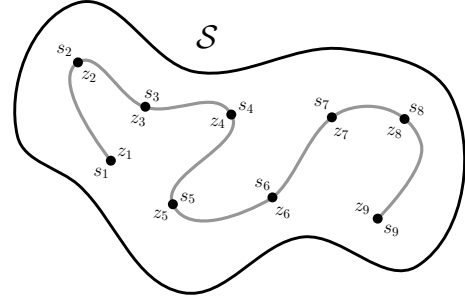


Fig. 3: The reduced state space model operates on the space $\tilde{\mathcal{S}} = \{s_1, s_2, \dots, s_T\}$ of visited trajectory states, yielding a finite-size description of the learning problem.

prior model to promote a certain type of state clustering. A reasonable choice is, for instance, to use a model which preferably groups “similar” states together (in other words, a model which favors clusterings that assign those states the same local control parameter). Similarity of states can be expressed, for example, by a monotonically decreasing decay function $f : [0, \infty) \rightarrow [0, 1]$ which takes as input the distance between two states. The pairwise distances can be in turn defined via some distance metric $\chi : \mathcal{S} \times \mathcal{S} \rightarrow [0, \infty)$.

Apart from the reasons listed in Section 2.2, there is an additional motivation, more intrinsically related to the dynamics of the system, why such a clustering can be useful: given that the transition model of our system admits locally smooth dynamics (which is typically the case for real-world systems), the resulting optimal system policy often turns out to be spatially smooth, too [27]. More specifically, under an optimal system policy, two nearby states are highly likely to experience similar controls, which is why it is reasonable to *a priori* assume that both share the same local control parameter. For the policy prediction task, it certainly makes sense to regularize our learning problem by encoding this particular structure of the solution space into our model.

We can express the prior probability of a certain clustering via the state similarity values, i.e. $d_{i,j} := \chi(s_i, s_j)$, $i, j \in \{1, \dots, |\mathcal{S}|\}$, for example, using a Potts model [28], i.e.

$$p_z(\mathbf{z}) \propto \prod_{i=1}^{|\mathcal{S}|} \exp\left(\frac{\beta}{2} \sum_{\substack{j=1 \\ j \neq i}}^{|\mathcal{S}|} f(d_{i,j}) \delta(z_i, z_j)\right).$$

Here, δ stands for Kronecker’s delta and $\beta \in [0, \infty)$ is called the inverse temperature of the model which controls the strength of the prior. Note that the Potts model is a special case of a Markov random field model [29] with clique factorization defined using pairwise potentials. From the prior model above we can easily derive the conditional distribution of a single indicator variable z_i , i.e.

$$p(z_i \mid z_{-i}) \propto \exp\left(\beta \sum_{\substack{j=1 \\ j \neq i}}^{|\mathcal{S}|} f(d_{i,j}) \delta(z_i, z_j)\right).^5 \quad (12)$$

This completes our inference framework for finite spaces.

5. Note that the scaling factor $\frac{1}{2}$ has vanished here due to the symmetry property of the metric χ .

2.3 Infinite state spaces

A major advantage of the clustering approach presented in the last section is that, due to the finite number of local policies to be learned from the limited amount of observation data, we can now apply the same methodology to infinite state spaces. This extension had been practically impossible for the static model due to the overfitting problem explained in Section 2.2. Nevertheless, there remains a fundamental conceptual problem: a straightforward extension of the model to infinite state spaces would imply that the distribution over possible state partitionings becomes an infinite-dimensional object (i.e. a distribution over functional mappings from states to local controls), requiring an uncountably infinite number of indicator variables. Certainly, such an object is non-trivial to handle computationally.

However, while the number of latent cluster assignments grows unbounded with the size of the state space, the amount of observed trajectory data always remains finite. A possible solution to the problem is therefore to reformulate the prediction task on a reduced state space $\tilde{S} = \{s_1, s_2, \dots, s_T\}$ containing only states along the observed trajectories, which always induces a model of finite size (see Fig. 3). More specifically, we consider only a finite set of indicator variables $\{z_t\}_{t=1}^T$, one for each expert state $s \in \tilde{S}$. Assuming that no state is visited twice, we may further use the same index set for both variable types.⁶ In order to limit the complexity of the dependency structure of the indicator variables for larger data sets, we generally let the value of indicator z_t depend only on a subset of the remaining variables \mathbf{z}_{-t} as defined by some neighborhood rule \mathcal{N} . The resulting joint distribution is then given as

$$p_z(\mathbf{z} | \mathbf{s}) \propto \prod_{t=1}^T \exp\left(\frac{\beta}{2} \sum_{t' \in \mathcal{N}_t} f(d_{t,t'}) \delta(z_t, z_{t'})\right),$$

which now implicitly depends on the state sequence \mathbf{s} through the pairwise distances $\{d_{t,t'}\}$, where $d_{t,t'} := \chi(s_t, s_{t'})$.

The use of a finite number of indicator variables along the expert trajectories obviously circumvents the above-mentioned problem of representational complexity. Nevertheless, there are some caveats associated with this approach. First of all, using a reduced state space model raises the question of marginal invariance: if we added a new trajectory point to the data set, would this change our belief about the previously visited states? In particular, how is this different from modeling that new point together with the initial ones in the first place? And further, what does such a model imply, in general, for unvisited states? Can we still make predictions about their local policies? These questions are in fact important if we plan to use our model to generalize the expert demonstrations to new situations, and hence they will be addressed in detail in Section 4.

Another (but related) issue is that we lose the simple generative interpretation of the model that could be used

⁶ Note that we make this assumption for notational convenience only and that it is not required from a mathematical point of view. Nonetheless, the assumption is reasonable as, in the infinite case, the event of reaching the exact same state twice has zero probability for most dynamic models. In the general case, however, the indicator variables require their own index set, ensuring that each state is associated with exactly one cluster, even when visited multiple times.

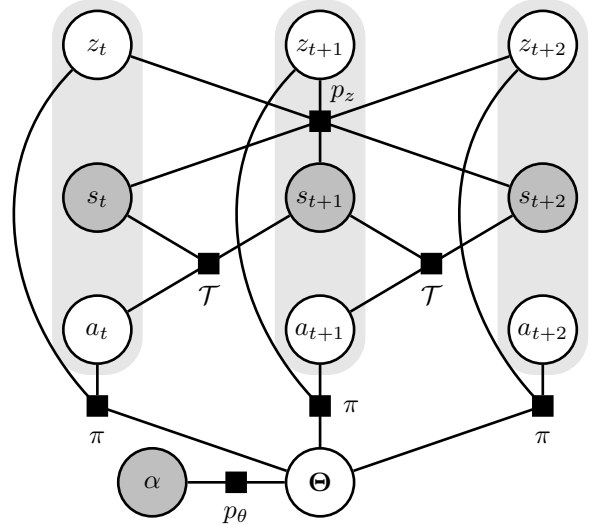


Fig. 4: Factor graph of the reduced state space model. The factors are defined by the same building blocks that were already used for the finite space model. The connections between the variables highlight their circular dependence. Observed variables are shaded in gray.

to explain the data generation beforehand. In the case of finite state spaces, we could think of a trajectory as being constructed by the following, step-wise mechanism: first, the prior $p_z(\mathbf{z})$ is used to generate a set of indicator variables for all states. Independently, we pick some value for α from $p_\alpha(\alpha)$ and sample K local control parameters from $p_\theta(\theta_k | \alpha)$. To finally generate a trajectory, we start with an initial state s_1 , generated by $p_1(s_1)$, pick a random action a_1 from $\pi(a_1 | s_1, \theta_{z_{s_1}})$ and transition to a new state s_2 according to $\mathcal{T}(s_2 | s_1, a_1)$, where we pick another action a_2 , and so on. Such a directed way of thinking is possible since the finite model naturally obeys a causal structure where later states depend on earlier ones and the decisions made there. Furthermore, the cluster assignments and the local controls could be generated in advance and isolated from each other because they were marginally independent according to the model.

For the reduced state space model, however, this interpretation no longer applies as the model has no natural directionality. In fact, its variables depend on each other in a cyclic fashion: altering the value of a particular indicator variable (say, the one corresponding to the last trajectory point) will have an effect on the values of all remaining indicators due to their spatial relationship encoded by the “prior distribution” $p_z(\mathbf{z} | \mathbf{s})$. Changing the values of the other indicators, however, will influence the actions being played at the respective states which, in turn, alters the probability of ending up with the observed trajectory in the first place and, hence, the position and value of the indicator variable we started with. A simple generative description of the model as in the finite case is therefore not possible.

Nevertheless, the individual building blocks of the model (that is, the policy, the transition model, etc.) together form a valid joint distribution which can be used for parameter inference. The structure of this reduced model

is depicted by the factor graph in Fig. 4 which highlights the circular dependence of the variables. Since we are not interested in predicting future state variables, it is sufficient to define our model in the form of a conditional distribution,

$$p(\mathbf{a}, \Theta, \mathbf{z} \mid \mathbf{s}, \alpha) = \frac{1}{Z} p_z(\mathbf{z} \mid \mathbf{s}) \prod_{k=1}^K p_{\theta}(\boldsymbol{\theta}_k \mid \alpha) \dots \\ \dots \times p_1(s_1) \prod_{t=1}^{T-1} \mathcal{T}(s_{t+1} \mid s_t, a_t) \pi(a_t \mid \boldsymbol{\theta}_{z_{s_t}}),$$

where we condition on the observed state sequence \mathbf{s} and denote by Z the corresponding normalizing constant. The good news is that there is no need to re-derive the corresponding sampling mechanisms as the conditional distributions of the remaining variables indeed remain unchanged. Recasting the inference problem as a finite-state problem on \tilde{S} thus effectively allows us to apply the exact same inference machinery that we already used for the finite space model.

3 NONPARAMETRIC POLICY RECOGNITION

In the last chapter, we presented a probabilistic policy recognition framework based on a finite mixture of K local policies, which we used to model an agent’s behavior. Basically, there are two cases when such a model is useful:

- either, we know the precise number of local policies
- or, irrespective of the true number of local policies, we want to find an approximate description of the agent behavior in terms of at most K distinct control situations (c.f. finite state controllers [26]).

In all other cases, we are faced with the non-trivial problem of choosing K . In fact, the choice of K should be considered as being more than just a mathematical necessity to perform inference with our model. As it determines the clustering structure of the state space in accordance with the demonstrated behavior, it directly controls the complexity class of inferred agent controllers. Therefore, by reasoning about the granularity of the partitioning based on the observed evidence, we can extract valuable information about the underlying control structure and state representation used by the agent. This offers a possibility to learn a task-appropriate description of the system state space from the expert data and, hence, the question of model complexity should be considered as part of the inference procedure itself.

From a machine learning perspective, there are two common ways to approach the problem. One is to apply model selection techniques in order to determine the most parsimonious model that is still in good agreement with the observed data. However, choosing a particular value for K also means that we consider only one possible explanation for the data, although other explanations might be likewise plausible. For many inference tasks, including this one, the more elegant approach is to let the number of clusters (i.e. local policies) be flexible by assuming a potentially infinite set of clusters, only a finite subset of which is then used to explain the particular data set at hand. This alternative way of thinking opens the door to the rich class of nonparametric models, which provide an integrated framework to formulate our inference problem over both model parameters and model complexity as a joint learning problem.

3.1 A Dirichlet process mixture model

The classical way to nonparametric clustering is to use a Dirichlet process mixture model (DPMM) [30]. These models can be obtained by starting with a finite mixture model and letting the number of mixture components (i.e. the number of local policies) approach infinity. In our case, we start with the clustering model of Section 2.2, using the mixing prior over indicator variables presented in Section 2.2.3, i.e.

$$\mathbf{q} \sim \text{DIR}(\mathbf{q} \mid \frac{\gamma}{K} \cdot \mathbf{1}^K) \quad z_i \mid \mathbf{q} \sim \text{CAT}(z_i \mid \mathbf{q}) \\ \boldsymbol{\theta}_k \sim \text{DIR}(\boldsymbol{\theta}_k \mid \alpha \cdot \mathbf{1}^{|\mathcal{A}|}) \quad a_t \mid s_t, \Theta, \mathbf{z} \sim \pi(a_t \mid \boldsymbol{\theta}_{z_{s_t}}) \quad (13) \\ s_1 \sim p_1(s_1) \quad s_{t+1} \mid s_t, a_t \sim \mathcal{T}(s_{t+1} \mid s_t, a_t).$$

From these equations, we arrive at the corresponding nonparametric model by letting K go to infinity. For the theoretical foundations of this limit, the reader is referred to the more general literature on Dirichlet Processes, such as [30], [31]. In this paper, we restrict ourselves to providing the required sampling mechanisms for the policy recognition problem.

In the infinite limit, the mixing proportions of the mixture components are marginalized out (that is, we use a collapsed sampler). The resulting distribution over partitionings is described by a Chinese restaurant process (CRP) [32] which can be derived, for instance, by considering the infinite limit $K \rightarrow \infty$ of the mixing process defined by the Gibbs sampling update in Eq. (11), i.e.

$$p(z_i = k \mid \mathbf{z}_{-i}, \gamma) \propto \begin{cases} \zeta_k^{(-i)} & \text{if } k \in \{1, \dots, K^*\}, \\ \gamma & \text{if } k = K^* + 1. \end{cases} \quad (14)$$

Here, K^* denotes the number of distinct entries in \mathbf{z}_{-i} which are represented by the numerical values $\{1, \dots, K^*\}$. According to the process, a state joins an existing cluster (i.e. a group of states whose indicators take the same value) with probability proportional to the number of members already in that cluster. Alternatively, it may create a new cluster with probability proportional to γ .

From the model equations in (13), it is evident that, given a particular setting of indicators which may now take arbitrary integer values, the conditional distributions of all other variable types remain unchanged as we only replaced the prior model $p_z(\mathbf{z})$ by the CRP. Hence, we can apply the same Gibbs updates for the action and control variables as before (irrespective of whether we operate on a finite or infinite state space) and only need to re-derive the conditional distributions for the indicator variables under consideration of the above defined process. According to Eq. (14), we herein need to distinguish whether an indicator variable takes a value already occupied by other indicators (i.e. it joins an existing cluster) or a new value (i.e. it creates a new cluster). Let $\{\boldsymbol{\theta}_k\}_{k=1}^{K^*}$ denote the set of control parameters associated with \mathbf{z}_{-i} . In the first case, that is, for $k \in \{1, \dots, K^*\}$, we then get

$$p(z_i = k \mid \mathbf{z}_{-i}, \mathbf{s}, \mathbf{a}, \{\boldsymbol{\theta}_{k'}\}_{k'=1}^{K^*}, \alpha, \gamma) \\ = p(z_i = k \mid \mathbf{z}_{-i}, \{a_t\}_{t:s_t=i}, \boldsymbol{\theta}_k, \alpha, \gamma) \\ \propto p(z_i = k \mid \mathbf{z}_{-i}, \boldsymbol{\theta}_k, \alpha, \gamma) p(\{a_t\}_{t:s_t=i} \mid z_i = k, \mathbf{z}_{-i}, \boldsymbol{\theta}_k, \alpha, \gamma) \\ \propto p(z_i = k \mid \mathbf{z}_{-i}, \gamma) \cdot p(\{a_t\}_{t:s_t=i} \mid \boldsymbol{\theta}_k) \\ \propto \zeta_k^{(-i)} \cdot \prod_{t:s_t=i} \pi(a_t \mid \boldsymbol{\theta}_k).$$

In the second case ($k = K^* + 1$), we instead obtain

$$\begin{aligned}
& p(z_i = K^* + 1 \mid \mathbf{z}_{-i}, \mathbf{s}, \mathbf{a}, \{\boldsymbol{\theta}_k\}_{k=1}^{K^*}, \alpha, \gamma) \\
&= p(z_i = K^* + 1 \mid \mathbf{z}_{-i}, \{a_t\}_{t:s_t=i}, \alpha, \gamma) \\
&\propto p(z_i = K^* + 1 \mid \mathbf{z}_{-i}, \alpha, \gamma) \dots \\
&\quad \dots \times p(\{a_t\}_{t:s_t=i} \mid z_i = K^* + 1, \mathbf{z}_{-i}, \alpha, \gamma) \\
&\propto p(z_i = K^* + 1 \mid \mathbf{z}_{-i}, \gamma) \cdot p(\{a_t\}_{t:s_t=i} \mid z_i = K^* + 1, \alpha) \\
&\propto \gamma \cdot \int_{\Delta} p(\{a_t\}_{t:s_t=i} \mid \boldsymbol{\theta}_{K^*+1}) p_{\theta}(\boldsymbol{\theta}_{K^*+1} \mid \alpha) d\boldsymbol{\theta}_{K^*+1} \\
&\propto \gamma \cdot \int_{\Delta} \prod_{t:s_t=i} \pi(a_t \mid \boldsymbol{\theta}_{K^*+1}) p_{\theta}(\boldsymbol{\theta}_{K^*+1} \mid \alpha) d\boldsymbol{\theta}_{K^*+1} \\
&\propto \gamma \cdot \text{DIRMULT}(\boldsymbol{\phi}_i \mid \alpha).
\end{aligned}$$

If a new cluster is created, we further need to initialize the corresponding control parameter $\boldsymbol{\theta}_{K^*+1}$ by performing the respective Gibbs update, i.e. by sampling from

$$\begin{aligned}
& p(\boldsymbol{\theta}_{K^*+1} \mid \mathbf{z}, \mathbf{s}, \mathbf{a}, \{\boldsymbol{\theta}_k\}_{k=1}^{K^*}, \alpha, \gamma) \\
&= p(\boldsymbol{\theta}_{K^*+1} \mid \{a_t\}_{t:z_{s_t}=K^*+1}, \alpha) \\
&\propto p_{\theta}(\boldsymbol{\theta}_{K^*+1} \mid \alpha) \cdot p(\{a_t\}_{t:z_{s_t}=K^*+1} \mid \boldsymbol{\theta}_{K^*+1}) \\
&\propto p_{\theta}(\boldsymbol{\theta}_{K^*+1} \mid \alpha) \cdot \prod_{t:z_{s_t}=K^*+1} \pi(a_t \mid \boldsymbol{\theta}_{K^*+1}) \\
&\propto \text{DIR}(\boldsymbol{\theta}_{K^*+1} \mid \boldsymbol{\xi}_{K^*+1} + \alpha \cdot \mathbf{1}^{|\mathcal{A}|}).
\end{aligned}$$

Should a cluster get unoccupied during the sampling process, the corresponding control parameter may be removed from the stored parameter set $\{\boldsymbol{\theta}_k\}$ and the index set for k needs to be updated. Note that this sampling mechanism is a specific instance of Algorithm 2 described in [30]. A collapsed variant can be derived in a similar fashion.

3.2 Policy recognition using the distance dependent Chinese restaurant process

In the previous section, we have seen that the DPMM can be derived as the nonparametric limit model of a finite mixture using a set of latent mixing proportions \mathbf{q} for the clusters. Though the DPMM allowed us to keep the number of active policies flexible and hence adaptable to the amount and complexity of the observed data, the CRP as the underlying clustering mechanism did not capture any spatial dependence between the indicators. In fact, in the CRP, the indicator variables are only coupled via their relative frequencies (see Eq. (14)) but not through their individual locations in space, which is why the resulting collection of random variables is inevitably exchangeable. In a sense, one could argue that the spatial structure of our prediction problem is *a priori* ignored.

The fact that DPMM models can be nevertheless used for spatial clustering tasks can be explained by the particular form of data likelihood models that are typically used for the mixture components. In a Gaussian mixture model [33], for instance, be it finite or infinite, the spatial clusters emerge due to the unimodal nature of the mixture components which in a way encodes the locality property of the model that is needed to obtain a meaningful spatial clustering of the data. For the policy recognition problem, however, since the clustering of states is performed at the level of the inferred action information (i.e. a grouping of states based on the current action samples, see Eq. (9)) and not on the

state sequence itself, the model is not able to exploit any spatial information via the likelihood model. Accordingly, we cannot expect to obtain any reasonable clustering of the state space, especially when the local policies are overlapping (i.e. when they share one or more common actions) and action information alone is not sufficient to discriminate between policies. In order to facilitate a spatially smooth clustering, we therefore need to incorporate the spatial information of the state sequence by considering non-exchangeable distributions over partitionings. More specifically, we should design our model in such a way that whenever a state s is “close” to some other state s' and assigned to some cluster \mathcal{C}_k then, *a priori*, s' should belong to the same cluster \mathcal{C}_k with high probability. In that sense, we are looking for a nonparametric counterpart of the Potts model.

One model with such property is the distance dependent Chinese restaurant process (ddCRP) [34].⁷ As opposed to the traditional CRP, the ddCRP explicitly takes into account the spatial structure of the data. This is done in the form of pairwise distances between states, which can be obtained, for instance, by defining an appropriate distance metric on the state space in the same way as we did for the Potts model. Instead of assigning states to clusters as done by the CRP, the ddCRP assigns states directly to other states according to their pairwise distances. More specifically, the probability that state i is assigned to state j is defined as

$$p(c_i = j \mid \mathbf{D}, \gamma) \propto \begin{cases} \gamma & \text{if } i = j, \\ f(d_{i,j}) & \text{otherwise,} \end{cases} \quad (15)$$

where \mathbf{D} denotes the collection of all pairwise distances, and c_i is the “to-state” assignment of state i which can be thought of as a directed edge on the graph defined on the set of all states in $\tilde{\mathcal{S}}$ (see Fig. 5). Accordingly, i and j in the above equation take the values $\{1, \dots, |\mathcal{S}|\}$ for the finite-space model and $\{1, \dots, T\}$ for our reduced state space model. The state clustering is then obtained as a byproduct of this mapping via the connected components of the resulting graph (see Fig. 5 again).

Replacing the CRP by the ddCRP and following the same line of argument as in [34], we obtain the required conditional distribution for the Gibbs update of a state assignment as

$$p(c_i = j \mid \mathbf{c}_{-i}, \mathbf{s}, \mathbf{a}, \alpha, \gamma) = \begin{cases} \gamma & j = i, \\ f(d_{i,j}) & \text{no clusters merged,} \\ f(d_{i,j}) \cdot \mathcal{L} & \mathcal{C}_{z_i} \text{ and } \mathcal{C}_{z_j} \text{ merged,} \end{cases}$$

where we used the shorthand notation

$$\mathcal{L} = \frac{\text{DIRMULT}(\boldsymbol{\xi}_{z_i} + \boldsymbol{\xi}_{z_j} \mid \alpha)}{\text{DIRMULT}(\boldsymbol{\xi}_{z_i} \mid \alpha) \text{DIRMULT}(\boldsymbol{\xi}_{z_j} \mid \alpha)}$$

for the data likelihood term. The $\xi_{k,j}$'s are defined as in Eq. (8) but are based on the clustering which arises when we ignore current link c_i . The resulting Gibbs sampler is a collapsed one as the local control parameters are necessarily marginalized out during the inference process.

⁷ While the authors in [34] avoid calling this model nonparametric since it cannot necessarily be cast as a mixture model originating from a random measure, we stick to this term to highlight the fact that there is no parameter K for the number of local controls, and to make a clear distinction to the parametric models in Section 2.

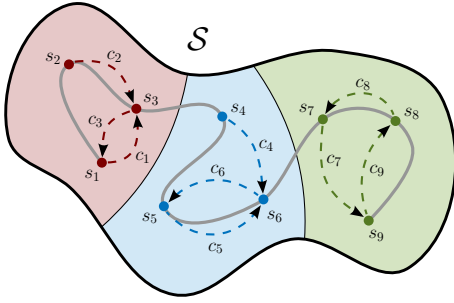


Fig. 5: Schematic illustration of the ddCRP-based clustering model. Each trajectory state is connected to some other state of the sequence. The resulting connected sub-graphs define the clustering. Coloring of the background illustrates the corresponding spatial cluster prediction (see Section 4).

4 PREDICTION, MARGINAL INVARIANCE & CONTROL IN INFINITE SPACES

When we extended our reasoning to infinite state spaces in Section 2.3, we inevitably arrived at the following questions: by modeling only states along observed trajectories, what can we say about the remaining states of the state space? Can we still use our model to make predictions about their local policies? It turns out that these questions are strongly related to what is known as *marginal invariance* [34] (sometimes also referred to as *marginalization property* or simply *consistency* [35]), a property which states that, simply put, a model is consistent in the sense that it always provides the same answer for any subset of its variables, no matter which size of the model we start with.

For our spatial models, that is, the Potts model and the ddCRP, it can be shown that this consistency property is lacking (see [34] for a detailed discussion), which means that we cannot expect to get compatible results if we perform our reduced model inference on two data sets of different sizes. On the contrary, making predictions for a new state would always require to re-run our Gibbs sampler on the augmented data set including that additional state. This brings us to the following practical dilemma: imagine an on-line policy recognition scenario where we observe an expert controlling our system. After a certain period of time, we are asked to take over control, using the experience we have acquired during the observation period. Each control command, whether performed by the expert or by us, will trigger a new state transition, meaning that new data points arrive sequentially one after another. Consequently, it is impossible to decide in advance which states to include in our reduced space \tilde{S} and which not to include. A rigorous approach would thus require to re-calibrate the model after each state transition – a costly operation.

On the other hand, it is evident that the resulting data set is naturally divided into two disjoint parts, namely the expert demonstrations and the subsequent states reached during the execution of the learned policy. Clearly, transitions occurring after the learning phase should by no means affect our belief about the expert policy and hence they should be completely discarded from the model. The easiest way to achieve this is indeed to “freeze” the model after the demonstration phase and to use the learned parameters to

extrapolate the gathered information to surrounding states. This can be done, for instance, by retaining the structure of our prior model to compute the resulting *maximum a posteriori* estimate for the extrapolated indicators of the new states based on the trained model. In the case of the ddCRP (Eq. (15)), this coincides with the nearest-neighbor estimate,

$$\hat{c}_{\text{new}} = \arg \max_k f(d_{k,\text{new}}) = \arg \min_k d_{k,\text{new}}.$$

Herein, $d_{k,\text{new}}$ denotes the distance of the new state to the k^{th} trajectory point. Now, one could argue that, in a sense, the comfort of retaining the finite model structure for infinite spaces came at the cost of not being able to compute the true posterior predictive distribution. Nonetheless, the reduced state space approach allows us to incorporate the spatial information of the data in a fairly natural manner (i.e. in the form of pairwise distances), enabling an easy way of modeling the data. Furthermore, the results in the next section demonstrate that the reduced model is, in principle, able to capture the relevant spatial properties of a system sufficiently accurate in order to make profound predictions about unseen states. Whether there exist alternative tractable models with similar properties remains to be seen.

5 SIMULATION RESULTS

For demonstration purposes, we focus on the case of continuous system dynamics which we consider to be more challenging than discrete dynamics for reasons explained in the previous sections. Herein, one of our goals is to assess the generalization abilities of the presented models by comparing their spatial prediction accuracies.

As a prototypical example, we consider a dynamical system which describes the circular motion of an agent on a two-dimensional state space. The action set of the agent consists of 24 distinct actions corresponding to rotated directions that divide the space of possible angles $[0, 2\pi)$ into equally-sized intervals. More specifically, action j corresponds to the angle $(j - 1) \frac{2\pi}{24}$ (see Fig. 6b). The transition model of the system is defined as follows: for each selected action, the agent makes a step of length $\mu = 1$ in the indicated direction. The so-obtained position is then distorted by additive zero-mean isotropic Gaussian noise of variance σ^2 . This defines our transition kernel as

$$p(s_{t+1} | s_t, a_t = j) = \mathcal{N}(s_{t+1} | s_t + \mu \cdot \mathbf{e}_j, \sigma^2 \mathbf{I}),$$

where $s_t, s_{t+1} \in \mathbb{R}^2$, \mathbf{e}_j denotes the two-dimensional unit vector pointing in the direction of action j , and \mathbf{I} is the two-dimensional identity matrix. The overall goal of our agent is to describe a circular motion around the origin in the best possible manner allowed by the specified actions. However, due to its limited sensory information, the agent can not observe its exact position on the plane but only distinguish between certain regions of the state space as illustrated by Fig. 6a. Also, the agent is unsure about the optimal control strategy, i.e. it does not always make an optimal decision but selects its actions uniformly at random from a subset of actions, consisting of the optimal one and the two actions pointing to neighboring directions (see Fig. 6a again). In order to render the scenario more interesting, we further let the agent change the direction of travel whenever the

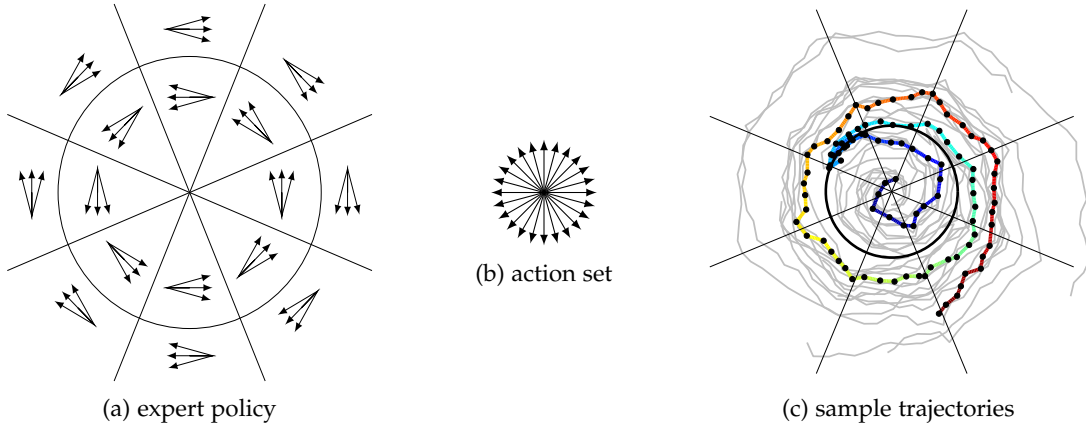


Fig. 6: (a) Schematic illustration of the expert policy which utilizes eight local controllers applied to sixteen distinct regions. (b) Action set available to the expert. (c) Example data set used for evaluation. One trajectory is highlighted in color.

critical distance of $r = 5$ to the origin is exceeded, so that each local policy is utilized in two distinct regions.

Having defined the expert controller in this way, we generate 10 sample trajectories per experiment, each of length $T = 100$. Herein, we assume a motion noise level of $\sigma = 0.2$ and initialize the agent's position uniformly at random on the unit circle. An example data set is shown in Fig. 6c. The trajectory data is then fed into the different inference algorithms to approximate the posterior distribution over expert controllers, and the whole experiment is repeated in 100 Monte Carlo runs.

For the spatial models, we use the Euclidean metric to compute the pairwise distances between states, i.e.

$$\chi(x, y) = \|x - y\|_2.$$

The similarity values are calculated using a Gaussian-shaped kernel. More specifically,

$$f_{\text{Potts}}(d) = \exp\left(-\frac{d^2}{\sigma_f^2}\right)$$

for the Potts model and

$$f_{\text{ddCRP}}(d) = (1 - \epsilon)f_{\text{Potts}}(d) + \epsilon$$

for the ddCRP model, with a constant offset of $\epsilon = 0.01$ to ensure that states with large distances can still join the same cluster. For the Potts model, we further use a neighborhood structure containing the eight closest trajectory points of a state in order to ensure that, in principle, each local policy may occur at least once in the neighborhood of a state. The concentration parameter for the local controls is set to $\alpha = 1$, corresponding to a uniform prior belief over local policies.

A major drawback of the Potts model is that posterior inference about the temperature parameter β turns out to be complicated due to the nonlinear effect of the parameter on the normalization of the model. Therefore, we manually selected a temperature of $\beta = 1.6$ based on a minimization of the average policy prediction error (discussed below) via parameter sweeping. As opposed to this, we extended the inference problem for the ddCRP to the self-link parameter γ as suggested in [34]. For this, we used an exponential prior, i.e.

$$p_\gamma(\gamma) = \text{EXP}(\gamma | \lambda),$$

with rate parameter $\lambda = 0.1$, and applied the independence Metropolis-Hastings algorithm [36] using $p_\gamma(\gamma)$ as proposal distribution and the initial value $\gamma = 1$. In all our simulations, the sampler quickly converged to its stationary distribution, yielding posterior values for γ with a standard deviation of 0.027 around the mean value 0.029.

To locally compare the true and the predicted policy at a given state, we computed their earth mover's distance (EMD) [37] with a ground distance metric measuring the angular distances of the involved actions. More precisely, we defined the distance between two actions i and j as the number of hops from arrow i to arrow j in Fig. 6b, i.e.

$$\chi_{\mathcal{A}}(i, j) = \min(|i-j|, |i-1|+|j-1|+1, |j-1|+|i-|\mathcal{A}||+1).$$

To track the learning progress of the algorithms, we calculated the average EMD over all states of a given trajectory set at each Gibbs iteration. Herein, the local policy predictions were computed from the single Gibbs sample of the respective iteration, consisting of all sampled actions, indicators and - in case of non-collapsed sampling - the local control parameters. The resulting mean EMDs and standard deviations are depicted in Fig. 7. The inset further shows the average EMD at non-trajectory states for the region depicted in Fig. 9a, reflecting the quality of the resulting spatial prediction. As expected, the finite Dirichlet model using a mixing prior ($\gamma = 1$) and the true number of local policies cannot provide any reasonable policy information as it does not exploit the spatial structure of the data. The resulting prediction error shows only a slight improvement as compared to an untrained model. Accordingly, we omit the graph for the Dirichlet process model which is faced with the even harder problem of additionally inferring the number of local policies. As opposed to the naive models, all spatial models capture the patterns in the data set reasonably well. In agreement with our reasoning in Section 2.1.2, we further observe that the collapsed Potts-Dirichlet mixture models has significantly faster mixing properties and a reduced prediction variance as compared to the non-collapsed version. However, the ddCRP model gives the best result, both in terms of mixing speed (see [34] for an explanation of this phenomenon) and model accuracy. Interestingly, this is despite the fact that the ddCRP model

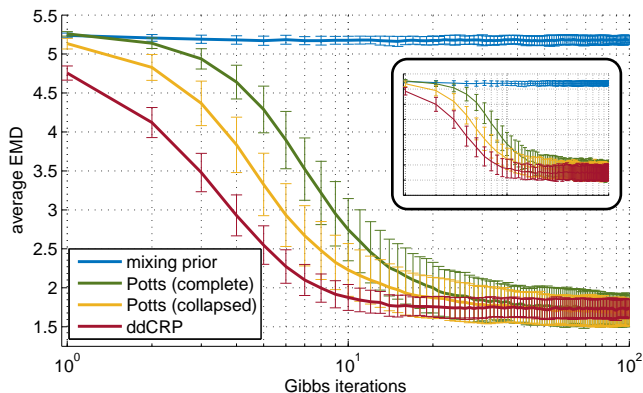


Fig. 7: Average policy prediction error at the simulated trajectory states (main figure) and at the non-trajectory states depicted in Fig. 9a (inset). Shown are the empirical means and standard deviations for all Gibbs iterations, computed from 100 Monte Carlo runs.

additionally needs to infer the number of local policies necessary to reproduce the expert behavior, indicating an overall good model fit. The posterior distribution over the number of local policies utilized by the model is depicted in Fig. 9c, which shows a pronounced peak at the true number used for data generation. A posterior sample of the control parameters is visualized in Fig. 8, which reveals that all basic motion patterns could be extracted by our algorithm.

Figure 9a visualizes the spatial prediction error of the ddCRP model in the form of a heat map by comparing the expert policy at non-trajectory points with the corresponding mean predictions, again in terms of their EMD. For this result, we focus on the ddCRP framework as it gave the best overall prediction result in terms of the average spatial prediction error (see inset in Fig. 7). As we would expect, the error is highest at the policy boundaries but comparably small within the policy regions, again indicating a good model fit. Note that the windmill shape of the error can be explained by the inherent asymmetry of the data generation scheme.⁸ Finally, we can observe that the variation of the error reaches its maximum at the transition regions (Fig. 9b) and generally grows with the distance to the supporting trajectory data, reflecting the increasing prediction uncertainty at regions far from the expert demonstrations.

6 DISCUSSION

In this work, we have proposed a novel approach to the LfD problem by jointly learning the latent control strategy of an observed expert demonstrator together with a task-appropriate representation of the system state space. We have seen that, when applied to a partially observable setting, the partitioning task can be interpreted as the process of learning the latent observation space of the demonstrator. With the described parametric and nonparametric models, we have presented two formulations of the same problem

8. Regions containing trajectories endings are locally underrepresented by the trajectory data which increases the chance of assigning the last trajectory points to the cluster of the preceding region, resulting in a smearing of that cluster into the next region.

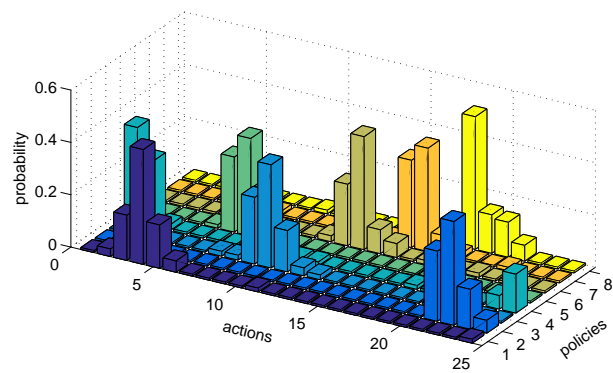


Fig. 8: Mean estimate of the local policies computed from the action and indicator samples of a single Gibbs sample which is drawn from the posterior distribution learned by the ddCRP model. The estimate reveals the eight local policies that had been used for data generation.

that can be either used to learn a global system controller of specified complexity, or to infer the required complexity from the observed expert behavior itself. Simulation results on a synthetic two-dimensional problem demonstrated the general applicability of our framework.

Due to the large body of literature on LfD, we can discuss only a small excerpt of the work that is related to ours, apart from what has been already mentioned in the introduction. In their early work, the authors of [38] presented a simple method to partition a system’s state space into a set of so-called *control situations* to learn a global controller based on a smaller set of informative states. Though the underlying clustering idea is quite similar to ours, their framework does not incorporate any demonstration data and the proposed partitioning is based on simple heuristics. A partitioning utilizing expert demonstrations is shown in [27] but the proposed expectation-maximization framework applies to deterministic policies and discrete spaces only. In the context of reinforcement learning, we further point to the work presented in [39] which follows a nonparametric philosophy similar to ours, to learn a distribution over predictive state representations for the decision-making problem. However, the closest methods to ours can be probably found in [18] and [10]. The authors of [18] presented a nonparametric inverse reinforcement learning approach to cluster the expert data based on a set of learned subgoals encoded in the form of local rewards. Yet, their method ignores the spatial structure of the data and can therefore hardly generalize to unvisited states. Moreover, the algorithm requires an MDP solver which renders a direct transfer to continuous settings difficult. The sub-intentional model in [10], on the other hand, can be used to learn a class of finite state controllers directly from the expert demonstrations. Also, the framework can handle various kinds of uncertainty about the data but, again, it is limited to discrete settings.

REFERENCES

- [1] B. D. Argall, S. Chernova, M. Veloso, and B. Browning, “A survey of robot learning from demonstration,” *Robotics and Autonomous Systems*, vol. 57, no. 5, pp. 469–483, 2009.

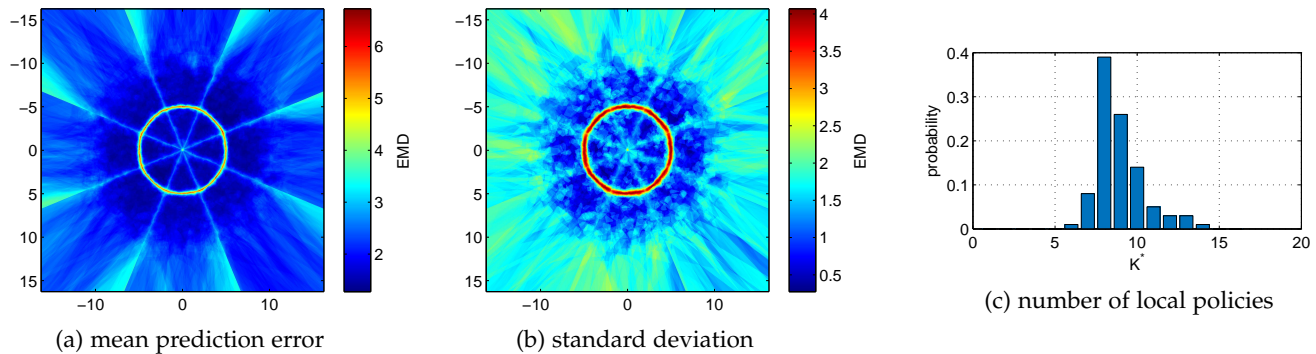


Fig. 9: Simulation results of the ddCRP model for the task illustrated in Figure 6a. All results are based on 100 Monte Carlo experiments. a) Mean values of the spatial policy prediction error. b) Standard deviation of the spatial policy prediction error. c) Posterior distribution over the number of local policies.

- [2] M. P. Deisenroth, D. Fox, and C. E. Rasmussen, "Gaussian processes for data-efficient learning in robotics and control," *IEEE Transactions on Pattern Analysis and Machine Intelligence*, vol. 37, no. 2, pp. 408–423, 2015.
- [3] P. Abbeel and A. Y. Ng, "Exploration and apprenticeship learning in reinforcement learning," in *Proc. 22nd International Conference on Machine Learning*. ACM, 2005, pp. 1–8.
- [4] D. Michie, M. Bain, and J. Hayes-Miches, "Cognitive models from subcognitive skills," *IEE Control Engineering Series*, vol. 44, pp. 71–99, 1990.
- [5] C. Sammut, S. Hurst, D. Kedzier, D. Michie et al., "Learning to fly," in *Proc. 9th International Workshop on Machine Learning, 1992*, pp. 385–393.
- [6] P. Abbeel, A. Coates, and A. Y. Ng, "Autonomous helicopter aerobatics through apprenticeship learning," *The International Journal of Robotics Research*, 2010.
- [7] D. A. Pomerleau, "Efficient training of artificial neural networks for autonomous navigation," *Neural Computation*, vol. 3, no. 1, pp. 88–97, 1991.
- [8] C. G. Atkeson and S. Schaal, "Robot learning from demonstration," in *Proc. 14th International Conference on Machine Learning (ICML)*, vol. 97, 1997, pp. 12–20.
- [9] P. Abbeel and A. Y. Ng, "Apprenticeship learning via inverse reinforcement learning," in *Proc. 21st International Conference on Machine Learning (ICML)*. ACM, 2004.
- [10] A. Panella and P. J. Gmytrasiewicz, "Nonparametric Bayesian learning of other agents' policies in interactive POMDPs," in *Proc. International Conference on Autonomous Agents and Multiagent Systems*, 2015, pp. 1875–1876.
- [11] A. Y. Ng, S. J. Russell et al., "Algorithms for inverse reinforcement learning," in *Proc. 17th International Conference on Machine Learning*, 2000, pp. 663–670.
- [12] D. Ramachandran and E. Amir, "Bayesian inverse reinforcement learning," *Proc. 20th International Joint Conference on Artificial Intelligence (IJCAI)*, vol. 51, pp. 2586–2591, 2007.
- [13] S. P. Singh, T. S. Jaakkola, and M. I. Jordan, "Learning without state-estimation in partially observable Markovian decision processes," in *ICML*, 1994, pp. 284–292.
- [14] J. Nash, "Non-cooperative games," *Annals of Mathematics*, pp. 286–295, 1951.
- [15] K. Hindriks and D. Tykhonov, "Opponent modelling in automated multi-issue negotiation using Bayesian learning," in *Proc. 7th International Joint Conference on Autonomous Agents and Multiagent Systems*, 2008, pp. 331–338.
- [16] R. S. Sutton and A. G. Barto, *Reinforcement learning: An introduction*. MIT press, 1998.
- [17] U. Syed and R. E. Schapire, "A game-theoretic approach to apprenticeship learning," in *Advances in Neural Information Processing Systems*, 2007, pp. 1449–1456.
- [18] B. Michini and J. P. How, "Bayesian nonparametric inverse reinforcement learning," in *Machine Learning and Knowledge Discovery in Databases*. Springer, 2012, pp. 148–163.
- [19] C. G. Atkeson and J. C. Santamaria, "A comparison of direct and model-based reinforcement learning," in *International Conference on Robotics and Automation*, 1997.
- [20] C. A. Rothkopf and C. Dimitrakakis, "Preference elicitation and inverse reinforcement learning," in *Machine Learning and Knowledge Discovery in Databases*. Springer, 2011, pp. 34–48.
- [21] O. Pietquin, "Inverse reinforcement learning for interactive systems," in *Proceedings of the 2nd Workshop on Machine Learning for Interactive Systems*. ACM, 2013, pp. 71–75.
- [22] S. Schaal, "Is imitation learning the route to humanoid robots?" *Trends in Cognitive Sciences*, vol. 3, no. 6, pp. 233–242, 1999.
- [23] K. Dvijotham and E. Todorov, "Inverse optimal control with linearly-solvable MDPs," in *Proc. 27th International Conference on Machine Learning*, 2010, pp. 335–342.
- [24] E. Charniak and R. P. Goldman, "A Bayesian model of plan recognition," *Artificial Intelligence*, vol. 64, no. 1, pp. 53–79, 1993.
- [25] B. Piot, M. Geist, and O. Pietquin, "Learning from demonstrations: Is it worth estimating a reward function?" in *Machine Learning and Knowledge Discovery in Databases*. Springer, 2013, pp. 17–32.
- [26] N. Meuleau, L. Peshkin, K.-E. Kim, and L. P. Kaelbling, "Learning finite-state controllers for partially observable environments," in *Proc. 15th Conference on Uncertainty in Artificial Intelligence*, 1999, pp. 427–436.
- [27] A. Šošić, A. M. Zoubir, and H. Koepl, "Policy recognition via expectation maximization," in *Proc. 41st IEEE International Conference on Acoustics, Speech and Signal Processing*, 2016.
- [28] R. B. Potts, "Some generalized order-disorder transformations," in *Mathematical Proceedings of the Cambridge Philosophical Society*, vol. 48, no. 01. Cambridge University Press, 1952, pp. 106–109.
- [29] D. Koller and N. Friedman, *Probabilistic Graphical Models: Principles and Techniques*. MIT press, 2009.
- [30] R. M. Neal, "Markov chain sampling methods for Dirichlet process mixture models," *Journal of Computational and Graphical Statistics*, vol. 9, no. 2, pp. 249–265, 2000.
- [31] T. S. Ferguson, "A Bayesian analysis of some nonparametric problems," *The Annals of Statistics*, pp. 209–230, 1973.
- [32] D. J. Aldous, *Exchangeability and related topics*. Springer, 1985.
- [33] C. E. Rasmussen, "The infinite Gaussian mixture model," in *Advances in Neural Information Processing Systems*. MIT Press, 2000, pp. 554–560.
- [34] D. M. Blei and P. I. Frazier, "Distance dependent Chinese restaurant processes," *The Journal of Machine Learning Research*, vol. 12, pp. 2461–2488, 2011.
- [35] C. E. Rasmussen, "Gaussian processes for machine learning." MIT Press, 2006.
- [36] S. Chib and E. Greenberg, "Understanding the Metropolis-Hastings algorithm," *The American Statistician*, vol. 49, no. 4, pp. 327–335, 1995.
- [37] Y. Rubner, C. Tomasi, and L. J. Guibas, "A metric for distributions with applications to image databases," in *6th International Conference on Computer Vision*, 1998. IEEE, 1998, pp. 59–66.
- [38] M. Waltz and K. Fu, "A heuristic approach to reinforcement learning control systems," *IEEE Transactions on Automatic Control*, vol. 10, no. 4, pp. 390–398, 1965.
- [39] F. Doshi-Velez, D. Pfau, F. Wood, and N. Roy, "Bayesian nonparametric methods for partially-observable reinforcement learning," *IEEE Transactions on Pattern Analysis and Machine Intelligence*, vol. 37, no. 2, pp. 394–407, 2015.